

## Effects of Build Orientation and Heat Treatment on Neutron Irradiation Hardening in Inconel 625 Fabricated via Laser Powder Bed Fusion

Mohanish Andurkar<sup>1</sup>, Valentina O'Donnell<sup>2</sup>, John Gahl<sup>2</sup>, Bart Prorok<sup>3</sup>, Tahmina Keya<sup>3</sup>, Greyson Harvill<sup>3</sup>, Scott Thompson<sup>1,\*</sup>

<sup>1</sup>Alan Levin Department of Mechanical and Nuclear Engineering, Kansas State University,  
Manhattan, Kansas, USA, 66506

<sup>2</sup>University of Missouri Research Reactor (MURR), University of Missouri, Columbia, Missouri,  
USA, 65211

<sup>3</sup>Department of Materials Engineering, Auburn University, Auburn, Alabama, USA, 36849

\*Corresponding author: smthompson@ksu.edu

### Abstract

Various Inconel 625 coupons fabricated via Laser Powder Bed Fusion (L-PBF) were neutron irradiated using the inside reflector of the reactor at the University of Missouri Research Reactor (MURR). Effects of build orientation and heat treatment on neutron-induced hardening were investigated by inspecting L-PBF samples built vertically or at a 45° angle in the following heat-treated conditions: as-built (no heat treatment), 700 °C for 1 hour, 900 °C for 1 hour, and 1050 °C for 1 hour. The microhardness results of L-PBF samples before and after neutron irradiation were compared with traditional wrought Inconel 625. All samples underwent an irradiation flux of  $6.61 \times 10^{13}$  neutrons/cm<sup>2</sup>/s for 310 hours for an estimated damage of 0.012 dpa. Results indicate that as-built L-PBF specimens are less prone to radiation hardening relative to their wrought counterparts. As-printed diagonal specimens were shown to harden by 8% as compared to 1.2% hardening in as-printed vertical specimens.

**Keywords:** Selective Laser Melting, Nickel Superalloy, Nuclear Radiation Damage, Vickers Microhardness, Additive Manufacturing

### Introduction

In recent decades, researchers have been working on building smaller, simpler, and more efficient nuclear reactors like Small Modular Reactors (SMR) and GEN IV reactors. Demand is high for structural materials used in building in-core and out-core components of GEN IV reactors that can withstand high operating temperatures and radiation doses to improve the life and safety of the reactor. Additive Manufacturing (AM) serves as a novel method to build complex-shaped components layer by layer with designed mechanical properties for higher temperatures. AM provides advantages compared to conventional machining like design flexibility, faster process setup, cost and waste reduction, and real time monitoring of microstructure and mechanical properties. A relatively mature and common technique for the AM of metals is laser-powder bed fusion (L-PBF) which employs 20-60 micron-thick layers of powder that is selectively melted

using a laser beam within an inert atmosphere. For L-PBF, un-melted powder can help support new layers, thus allowing for the manufacture of complex components like heat exchangers, cellular structures, and topology-optimized parts.

Nickel based superalloys are proposed to be utilized in GEN IV reactors [1]. One nickel-based superalloy, Inconel 625, possesses excellent high temperature strength, creep, and toughness. It is gaining significant importance to be utilized in next-generation nuclear reactors particularly in control rod and reactor core applications [2]. Inconel 625 is a solid solution strengthening alloy due to the presence of elements like Mo and Nb. Inconel 625 is becoming more ubiquitous in various industries like aerospace, nuclear or any other industries where harsh environments are expected [3]. Conventional machining methods often face difficulties in processing Inconel 625 components due to its high hardness, reduced machinability, and low thermal conductivity [4]. There have been various studies conducted in the past to understand the microstructure and mechanical properties of Inconel 625 built via different AM techniques. Fang et al. [5] studied the microstructure evolution of Inconel 625 components built via L-PBF that were subjected to different heat treatments. It was found that as-built specimens possessed higher hardness due to high dislocation density arising from high thermal gradients during the L-PBF process. The microhardness values decreased when the as-built specimens were subjected to heat treatment temperatures at 870, 980, and 1150 °C for 1 hour. The samples were furnace cooled to room temperature. The heat treatment reduced the dislocation density and increased homogenization of grains. Szmytka et al. [6] compared the mechanical properties of Inconel 625 fabricated via L-PBF and Laser Melting Deposition (LMD) – a Directed Energy Deposition (DED) AM method, as well as wrought. They found that as-built L-PBF and LMD specimens exhibited higher hardness values compared to wrought specimens. In addition, they discovered after performing a 1h heat treatment at 1100 °C, the hardness values decreased and thus the ductility of the specimens increased.

Neutron irradiation on metals induces defects like voids, interstitials, dislocations, swelling, helium embrittlement, and radiation induced hardening [7][8]. While there have been studies conducted in the past to investigate the influence of ion irradiation on AM Inconel metals, the effects of neutron irradiation on mechanical properties of AM Inconel 625 are still unclear [9][10]. Claudson studied the effects of neutron irradiation, with exposures exceeding >1 MeV, on the elevated temperature mechanical properties of wrought nickel-based and refractory metal alloys. The results showed a decrease in ductility at elevated temperatures compared to those measured at room temperature [11].

The aim of this paper is to investigate the effects of neutron irradiation on the hardness of wrought and AM Inconel 625. The AM Inconel 625 samples were built using two different build orientations (vertical and diagonal) via L-PBF. All L-PBF and wrought Inconel 625 samples were irradiated inside a 10 MW nuclear reactor for duration of 310 hours. During this irradiation, each sample experienced a neutron flux of  $6.61 \times 10^{13}$  neutrons/cm<sup>2</sup>/s. Out of this total flux, 90% was contributed by thermal neutrons and 10% by fast neutrons. The total flux corresponds to a displacements per atom (dpa) value of 0.012. The radiation induced hardening was measured using Vickers microhardness on all pre- and post-irradiated samples. Comparing the hardening behavior of additive manufactured components and wrought Inconel 625 under neutron irradiation provides

a better understanding on how AM and post processing affect the structural integrity of an important nickel-based superalloy under harsh environment.

### Methods

Plasma atomized, virgin Inconel 625 powder with a mean particle diameter of 31.31  $\mu\text{m}$  was supplied by Carpenter Technologies. The chemical composition of Inconel 625 powder used for L-PBF in this study, adhering to ASTM Standard for Additively Manufacturing Nickel Alloy UNS N06625, is presented in Table 1. Inconel 625 cubes of 10 mm<sup>3</sup> dimension were additively manufactured using a Concept Laser Mlab 100R system. The Concept Laser consists of a 100 W fiber laser with wavelength of 70 nm. The building process was carried out in an enclosed argon atmosphere for minimization of oxidization. Cubes were iteratively built at various process parameters and then inspected for density. Final process parameters provided for 99.79% dense samples, these process parameters were: power = 90 W, scan speed = 800 mm/s, laser diameter = 80  $\mu\text{m}$ , hatch spacing = 60  $\mu\text{m}$ , and a layer thickness = 25  $\mu\text{m}$ . For experimental control and baselining, wrought Inconel 625 plate (152.4 x 152.4 x 4.76 mm<sup>3</sup>) was procured from Metalmen, NY, USA. The plate was manufactured per AMS5599 specification. Small 1 x 1 x 0.5 mm<sup>3</sup> samples were sectioned from the plate using wire electrical discharge machining (EDM). The chemical composition of wrought Inconel 625 is indicated in Table 1.

Table 1: Elemental composition of L-PBF powder and wrought Inconel 625 (% in weight)

% wt.	Ni	Cr	Mo	Fe	Nb+ Ta	Co	C	P	S	Al	Ti	Mn
UNS N06625	Bal	20-23	8-10	<5.0	3.15 -	<1	<0.1	<0.015	<0.015	<0.4	<0.4	<0.5
L-PBF	Bal	21.59	9.0	2.95	4.15 3.55	0.03	0.04	<0.015	<0.015	0.11	0.11	<0.5
Wrought	Bal	22.36	9.0	0.72	3.32	0.8	0.03	0.009	0.005	0.08	0.3	0.18

The L-PBF Inconel 625 samples were printed in two orientations i.e., Vertical (V), and Diagonal (D) as presented in Fig. 1. An island scanning strategy with a checkerboard pattern consisting of 5 x 5 mm squares was used. Each island alternated the scan direction perpendicular with-respect-to adjacent islands. Both vertical and diagonal samples were separated from the build plate via wire EDM and then subjected to various heat treatments. The V and D Inconel 625 samples were subjected to three heat-treatment temperatures of 700 °C, 900 °C, and 1050 °C for 1 hour. The rationale behind selecting these temperatures was to form the  $\delta$  phase in the additively manufactured IN625; as shown in a TTT diagram provided by National Institute of Standards and Technology (NIST) [12]. Wrought Inconel 625 samples were subjected to the same heat-treatment temperatures for 40 hours. Some L-PBF specimens were not heat treated, i.e., left in the as-built condition. Heating ramps used during heat treatment were ~5 °C/min. All specimens were subjected to air cooling to room temperature while remaining in the furnace. Uncertainty in heat treatment temperatures is  $\pm 5$  °C. For each sample, 5 microhardness measurements were taken on surfaces indicated in Fig. 1 using a Phase II 900-391D microhardness tester to be able to calculate average and standard deviation in measurements. Error bars on the plots represent the standard

deviation. The indentations were made using a 1 kgf (9.8 N) load applied with a 15 secs dwell time.



Figure 1: Vertically and diagonally built L-PBF Inconel 625 samples on build platform. Red arrows indicate the face used to measure microhardness.

The samples were wrapped in aluminum foil and placed inside a 2.54 cm diameter vessel. The vessel was then placed into the reflector of the 10 MW reactor for 310 hours. All samples faced a total flux of  $6.61 \times 10^{13}$  neutrons/cm<sup>2</sup>/s which corresponds to a fluence of  $7.37 \times 10^{19}$  neutrons/cm<sup>2</sup>. The damage experienced by all samples was calculated to be 0.012 dpa. The microhardness measurements on radioactive samples were performed inside a hot cell equipped with manipulator arms as shown in Fig. 2.

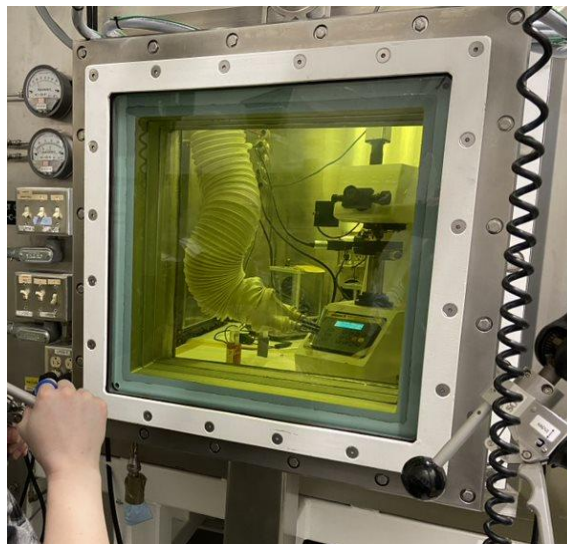


Figure 2: Hot cell with manipulator arms for performing microhardness measurements of radioactive Inconel 625 samples.

## Results and Discussions

The Vickers microhardness values of the as-built, pre-irradiated L-PBF Inconel 625 samples (built in vertical and diagonal directions) are shown in Fig. 3. For the vertical and diagonal samples, the microhardness values were measured to be  $364 \pm 1.175$  HV and  $359.25 \pm 2.625$  HV, respectively. The two different build orientations showed minimal variation in microhardness indicating directional independency in hardness of the L-PBF Inconel 625. This observation is consistent with past research conducted by Wang et al. on Inconel 718 [13]. As-built L-PBF Inconel 625 samples showed superior microhardness compared to as-received wrought Inconel 625 which had a microhardness of  $243.85 \pm 1.15$  HV. The higher microhardness in L-PBF samples is due to them having fine dendritic microstructure and high dislocation densities arising from high thermal gradients and cooling rates ( $\sim 10^5$  K/s) imposed by the fast-moving, high-heat-flux laser during the L-PBF process. The high cooling and solidification rates help in trapping the heavy atoms like Molybdenum (Mo) and Niobium (Nb) along interdendritic boundaries. These heavy atoms located along sub domain boundaries restrict the sliding of dislocations under external stress which ultimately increases the hardness of the material. The lower hardness of the as-received wrought Inconel 625 is due to it possessing a more homogenous microstructure with equiaxed grains due to prolonged heat treatment and lower dislocation density. In addition, there is less segregation of heavy atoms like Mo and Nb along the grain boundaries since the amount of Nb in the wrought samples was less than that of the L-PBF Inconel 625 powder. The higher standard deviation in microhardness for the L-PBF samples may be due to them possessing a less homogeneous and highly textured microstructure and the micro segregation of heavy atoms like Nb and Mo in the microstructure.

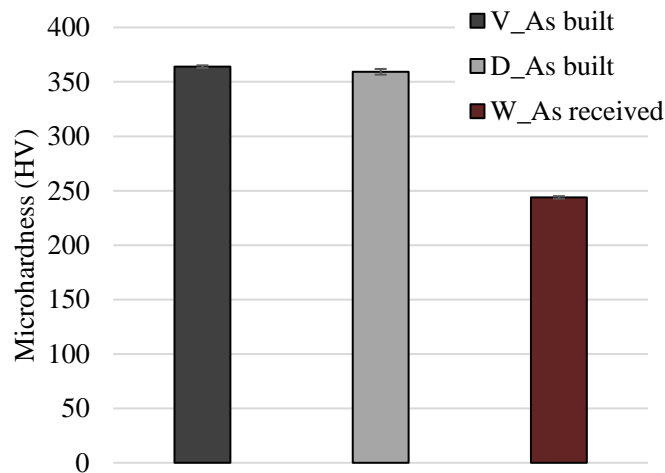


Figure 3: Microhardness of pre-irradiated Inconel 625 samples, including as-built/L-PBF vertical (V), as-built/L-PBF diagonal (D), and wrought (W). Error bars represent standard deviation.

Performing heat treatments on the as-built L-PBF Inconel 625 samples was found to decrease microhardness. As presented in Fig. 4, increasing the heat-treatment temperature resulted in reduction of sample microhardness. Performing the same heat treatment process on wrought Inconel 625 showed different trends compared to L-PBF Inconel 625. The slight decrease in microhardness from the as-built state to 700 °C for the vertically-built L-PBF Inconel 625 sample is potentially due to a reduction in dislocation density and relaxation of micro strains. Interestingly,

heat treating the L-PBF samples at 1050 °C brought their hardness values closer to that of the as-received wrought Inconel 625. The reduction in microhardness after heat treatment is most likely due to a decline in dislocation densities, solid state transformations, grain recrystallization or grain coarsening, and micro stress relaxation. Similar results were conveyed in past studies [5]. The microhardness increased when wrought Inconel 625 was heat treated at 900 °C and 1050 °C. The likely reason for this is the onset of  $\gamma''$  and  $\delta$  intermetallic phases forming in small amounts along sub-grain domain boundaries.

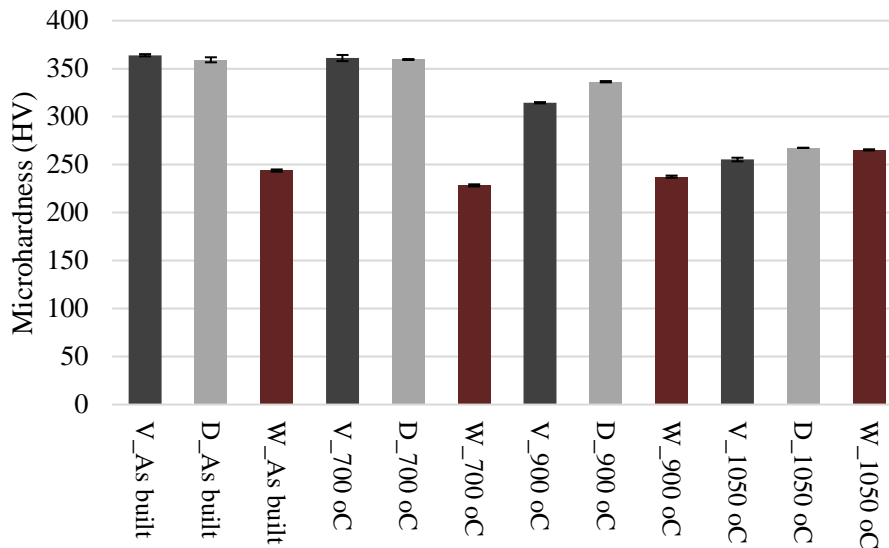


Figure 4: Pre-irradiation microhardness measurements of as-built and heat-treated vertical (V) (dark grey) and diagonal (D) (light grey) L-PBF Inconel 625 samples and wrought (W) (dark red) Inconel 625 samples.

The microhardness values of L-PBF and wrought Inconel 625 samples after thermal neutron irradiation are presented in Fig. 5. It can be observed that neutron irradiation induced hardening occurred in all L-PBF and wrought Inconel 625 samples. Irradiation induced hardening was more prominent in the as-built diagonal L-PBF samples compared to the vertical-built samples. As-built diagonal L-PBF sample microhardness increased ~8% compared to only 1.2% in the as-built vertical L-PBF samples as presented in Fig. 6. It is hypothesized that the diagonal specimen layer-to-layer porosity and grain orientation are slightly different than that of the vertical specimens due to how they were oriented and manufactured (i.e., layer-wise scan strategy) during L-PBF. The smaller error bars shown in Fig. 5 for wrought Inconel 625, as compared to the L-PBF samples, suggest more homogeneity in microstructure and mechanical properties post irradiation in wrought Inconel 625. Heat treated vertical L-PBF and wrought samples at 1050 °C underwent slight softening as shown by negative percent change in Fig. 6. This may be due to the dissolution of precipitates like  $\gamma''$  and  $\delta$ , which primarily consist of Nb and Mo elements, that formed along sub domain grain boundaries. These precipitates restrict the movement of dislocations under external stress. Similar observations have been reported in past studies [14]–[16]. From Fig. 6, it is observed that all L-PBF Inconel 625 samples possessed better resistance to radiation induced hardening compared to all wrought Inconel 625 samples.

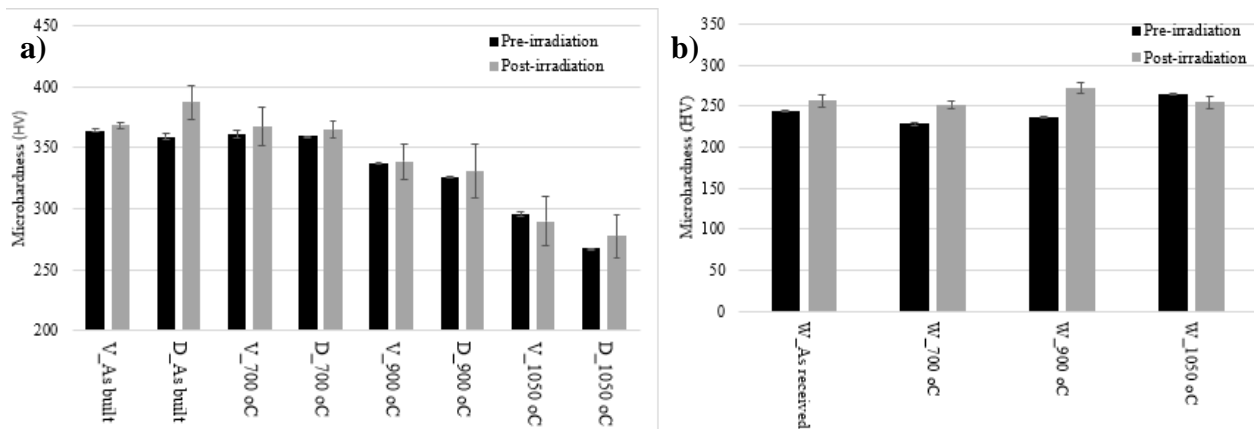


Figure 5: Pre and post thermal neutron irradiation microhardness measurements of (a) all L-PBF Inconel 625 specimens built in vertical and diagonal orientations and (b) all wrought Inconel 625 samples.

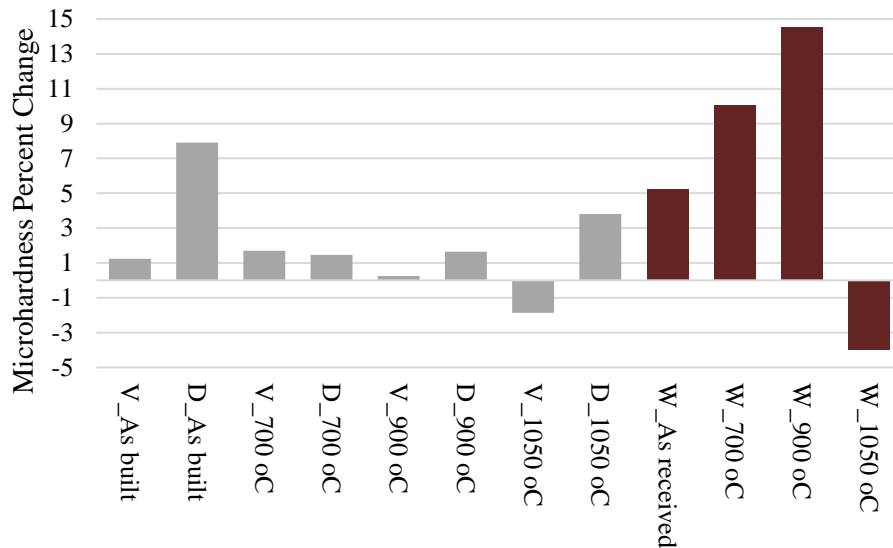


Figure 6: Percent change in microhardness of as-built and heat-treated vertically (V) and diagonally (D) printed L-PBF and wrought (W) Inconel 625 samples after neutron irradiation.

### Conclusions

L-PBF Inconel 625 samples built in two different directions in the as-built and heat-treated conditions were successfully irradiated within a 10 MW nuclear reactor to study the phenomenon of neutron irradiation hardening. The method of measuring microhardness of radioactive samples was established by using a hot cell and manipulator arms. Primary findings noted from this study are summarized below:

- The as-built vertical and diagonal L-PBF Inconel 625 samples had higher pre-irradiation hardness values compared to the as-received wrought Inconel 625 samples.

- The employed heat treatments used on the vertically- and diagonally-built L-PBF Inconel 625 samples decreased their microhardness as the temperature increased from 700 °C to 1050 °C. The heat treatment process brought down the microhardness of L-PBF Inconel 625 imitating that of wrought Inconel 625.
- Even after modest neutron irradiation, all samples, except the vertically-built 1050 °C heat treated L-PBF and wrought 1050 °C heat treated samples, experienced neutron irradiation hardening.
- The as-built vertical L-PBF sample underwent less hardening (1.2%) than the as-built diagonal L-PBF sample (8%) indicating potential orientation effects. As-received wrought samples faced 5.25% radiation induced hardening.
- The L-PBF Inconel 625 samples displayed more resistance to radiation hardening (lower percent change) as compared to wrought Inconel 625 samples (higher percent change).

This study has provided more data indicating the structural integrity of components made from AM when exposed to full-spectrum nuclear radiation. Results provide insight into how one may minimize radiation hardening in additive manufactured materials for maintaining material property constraints. The results herein should assist engineers in selecting an appropriate heat treatment for additive manufactured nickel-based superalloys for increased radiation resistance. Results should increase confidence levels for adopting AM for building nuclear reactor components which perform the same or better than conventionally manufactured components.

### **Acknowledgement**

This material is based upon work supported by the U.S. Department of Energy’s Office of Nuclear Energy under Award Number DE-NE0008865.

### **Disclaimer**

This report was prepared as an account of work sponsored by an agency of the United States Government. Neither the United States Government nor any agency thereof, nor any of their employees, makes any warranty, express or implied, or assumes any legal liability or responsibility for the accuracy, completeness, or usefulness of any information, apparatus, product, or process disclosed, or represents that its use would not infringe privately owned rights. Reference herein to any specific commercial product, process, or service by trade name, trademark, manufacturer, or otherwise does not necessarily constitute or imply its endorsement, recommendation, or favoring by the United States Government or any agency thereof. The views and opinions of authors expressed herein do not necessarily state or reflect those of the United States Government or any agency thereof.

### **References**

- [1] A. F. Rowcliffe, L. K. Mansur, D. T. Hoelzer, and R. K. Nanstad, “Perspectives on radiation effects in nickel-base alloys for applications in advanced reactors,” *Journal of Nuclear Materials*, vol. 392, no. 2, pp. 341–352, 2009, doi: 10.1016/j.jnucmat.2009.03.023.
- [2] M. A. Stopher, “The effects of neutron radiation on nickel-based alloys,” *Materials Science and Technology (United Kingdom)*, vol. 33, no. 5, pp. 518–536, 2017, doi:



10.1080/02670836.2016.1187334.

- [3] S. Li, Q. Wei, Y. Shi, C. K. Chua, Z. Zhu, and D. Zhang, “Microstructure Characteristics of Inconel 625 Superalloy Manufactured by Selective Laser Melting,” *Journal of Materials Science and Technology*, vol. 31, no. 9, pp. 946–952, 2015, doi: 10.1016/j.jmst.2014.09.020.
- [4] A. K. Parida and K. Maity, “Comparison the machinability of Inconel 718, Inconel 625 and Monel 400 in hot turning operation,” *Engineering Science and Technology, an International Journal*, vol. 21, no. 3, pp. 364–370, 2018, doi: 10.1016/j.jestch.2018.03.018.
- [5] C. Li, R. White, X. Y. Fang, M. Weaver, and Y. B. Guo, “Microstructure evolution characteristics of Inconel 625 alloy from selective laser melting to heat treatment,” *Materials Science and Engineering A*, vol. 705, no. August, pp. 20–31, 2017, doi: 10.1016/j.msea.2017.08.058.
- [6] J. Nguejio, F. Szmytka, S. Hallais, A. Tanguy, S. Nardone, and M. Godino Martinez, “Comparison of microstructure features and mechanical properties for additive manufactured and wrought nickel alloys 625,” *Materials Science and Engineering A*, vol. 764, no. July, 2019, doi: 10.1016/j.msea.2019.138214.
- [7] A. F. Rowcliffe, “Neutron irradiation facilities for fission and fusion reactor materials studies,” *Nuclear Inst. and Methods in Physics Research, A*, vol. 249, no. 1, pp. 26–33, 1986, doi: 10.1016/0168-9002(86)90238-X.
- [8] S. J. Zinkle and G. S. Was, “Materials challenges in nuclear energy,” *Acta Materialia*, vol. 61, no. 3, pp. 735–758, 2013, doi: 10.1016/j.actamat.2012.11.004.
- [9] I. Cieřlik, M. Duchna, T. Płociński, E. Wyszowska, A. Azarov, and M. Zieniuk, “Ion irradiation effect on the microstructure of Inconel 625 obtained by Selective Laser Melting and by the metallurgical process,” *Surface and Coatings Technology*, vol. 396, no. May, p. 125952, 2020, doi: 10.1016/j.surfcoat.2020.125952.
- [10] K. Kumar, C. Li, K. J. Leonard, H. Bei, and S. J. Zinkle, “Microstructural stability and mechanical behavior of FeNiMnCr high entropy alloy under ion irradiation,” *Acta Materialia*, vol. 113, pp. 230–244, 2016, doi: 10.1016/j.actamat.2016.05.007.
- [11] T. T. Claudson, “Effects of Neutron Irradiation on the Elevated Temperature Mechanical Properties of Nickel-Base and Refractory Metal Alloys,” *Effects of Radiation on Structural Metals*, pp. 67-67–28, 2009, doi: 10.1520/stp41318s.
- [12] M. R. Stoudt *et al.*, “The Influence of Annealing Temperature and Time on the Formation of  $\delta$ -Phase in Additively-Manufactured Inconel 625,” *Metallurgical and Materials Transactions A: Physical Metallurgy and Materials Science*, vol. 49, no. 7, pp. 3028–3037, 2018, doi: 10.1007/s11661-018-4643-y.
- [13] Z. Wang, K. Guan, M. Gao, X. Li, X. Chen, and X. Zeng, “The microstructure and mechanical properties of deposited-IN718 by selective laser melting,” *Journal of Alloys and Compounds*, vol. 513, pp. 518–523, 2012, doi: 10.1016/j.jallcom.2011.10.107.
- [14] Z. H. Ismail, “Effect of low dose neutron irradiation on the mechanical properties of an AlMgSi alloy,” *Radiation Effects and Defects in Solids*, vol. 112, no. 4, pp. 105–110, 1990,

doi: 10.1080/10420159008213036.

- [15] T. S. Byun *et al.*, “Mechanical behavior of additively manufactured and wrought 316L stainless steels before and after neutron irradiation,” *Journal of Nuclear Materials*, vol. 548, p. 152849, 2021, doi: 10.1016/j.jnucmat.2021.152849.
- [16] T. S. Byun and K. Farrell, “Tensile properties of Inconel 718 after low temperature neutron irradiation,” *Journal of Nuclear Materials*, vol. 318, no. SUPPL, pp. 292–299, 2003, doi: 10.1016/S0022-3115(03)00006-0.